

The Emission of Non-Thermal Microwave Radiation by a Martian Dust Storm

Christopher Ruf¹, Nilton O. Renno¹, Jasper F. Kok¹, Etienne Bandelier¹, Michael J.
Sander², Steven Gross¹, Lyle Skjerve², and Bruce Cantor³

1. Department of Atmospheric, Oceanic and Space Sciences, University of Michigan,
Ann Arbor, MI 48109 USA
2. Jet Propulsion Laboratory, California Institute of Technology, Pasadena, CA 91109
USA
3. Malin Space Science Systems, Inc., San Diego, CA 92191 USA

Correspondence should be addressed to: Nilton O. Renno, email: renno@alum.mit.edu

Submitted to Geophysical Research Letters

Revised on May 10, 2009

Abstract

We report evidence for the emission of non-thermal microwave radiation by a deep martian dust storm. The observations were made using an innovative detector that can discriminate between radiation of thermal and non-thermal origin by measuring the high order moments of its electric field strength. Measurements with this detector, installed in a 34 m radio telescope of the Deep Space Network (DSN), were made for about 5 hours a day over a dozen days between 22 May and 16 June 2006. Non-thermal radiation was detected, for a few hours only when a 35 km deep martian dust storm was within the field of view of the radio telescope on 8 June 2006. The spectrum of the non-thermal radiation has significant peaks around predicted values of the lowest three modes of the martian Schumann Resonance (SR). The SR results from electromagnetic standing waves formed in the concentric spherical cavity between the martian surface and its ionosphere and forced by large-scale electric discharge. Thus, the non-thermal radiation was probably caused by electric discharge in the martian dust storm.

1. Introduction

Large electric fields have been measured in terrestrial wind-blown sand, dust storms and dust devils [*Stow, 1969; Schmidt et al., 1998; Renno et al., 2004; Renno and Kok, 2008*]. There is both theoretical and observational evidence that martian dust storms also generate large electric fields [*Melnik and Parrot, 1998; Farrell et al., 1999; Renno et al., 2004*] and emit non-thermal microwave radiation [*Renno et al., 2003, 2004*]. These investigations, together with results of laboratory and field experiments conducted by our group in the past 7 years (Fig. S1) motivated the observations described in this article. At low spatial resolutions, it is difficult to distinguish thermal from non-thermal radiation by traditional power-based techniques because the intensity of thermal emission by the sensor (instrument noise) and by the planet itself are usually orders of magnitude larger than that of the planet's non-thermal radiation. An innovative microwave detector recently developed at the University of Michigan measures both the power of the signal and its kurtosis [*Ruf et al., 2006*]. The kurtosis is extremely sensitive to the presence of non-thermal radiation, but is insensitive to variations in the intensity of the thermal radiation or in the gain of a radiometer receiver. As a result, it is able to detect the presence of non-thermal radiation of much lower intensity than ordinary thermal radiation [*De Roo et al., 2007*].

2. Mars Observations

Observations of microwave emission by Mars were made from 22 May to 16 June 2006 using antenna DSS-13 of NASA's Deep Space Network (DSN). DSS-13 is a steerable 34 m diameter parabolic antenna with a low noise microwave transceiver.

Radiometric measurements were made using a channel of the receiver operating between 8470 and 8490 MHz. This spectrum was divided into 8 adjacent, 2.5 MHz wide, sub bands prior to kurtosis calculation. The angular resolution of the antenna at this frequency is ~ 200 arcsec, and the full Mars disk fills approximately 0.04% of the solid angle of the antenna beam.

Performance of the kurtosis detector on DSS-13 was evaluated using the Mars Reconnaissance Orbiter (MRO) communication link as a test beacon (Fig. S2). The results demonstrate that: a) the sinusoidal MRO signal lowers the kurtosis as expected [Ruf *et al.*, 2006] and only in one sub band; b) signal modulation such as that indicative of Schumann Resonance (SR) was not observed; and c) the standard deviation of the kurtosis in the absence of non-thermal signals is $\sigma_K = 0.03$ in all sub bands. This σ_K level is for a sample integration time of 4.2 ms and represents $N=27,000$ independent samples [De Roo *et al.*, 2007]. Any changes in kurtosis greater than ~ 0.1 (a $3\text{-}\sigma$ change) is statistically significant evidence of a non-thermal radiation.

During the three-week campaign, measurements were made at most opportunities when Mars was sufficiently high above the horizon at DSS-13, resulting in about 5 hours of observation per day on 12 days. Occasional non-thermal signals, probably due to terrestrial man-made sources, were detected. In each of these cases, the non-thermal kurtosis was isolated to only one or a few adjacent sub bands and the others maintained their thermal value (Fig. S2). The telescope was also routinely pointed slightly away from Mars to help differentiate between martian and terrestrial sources. On 8 June 2006, between 19:14 and 22:40 UTC, an unusual pattern of non-thermal radiation was detected in all 8 sub bands and only when the antenna was pointed at Mars. This was also the only

time during the 12 days of observations in which a deep convective dust storm capable of producing large electric fields [*Melnik and Parrot, 1998; Kok and Renno, 2009*] was observed in images of Mars Global Surveyor's Mars Observation Camera (MOC). An image of this convective dust storm is shown in Fig. 1.

Fig. 2 shows a sample of the kurtosis measured between 19:20:00 and 19:20:30 UTC on 8 June 2006. Individual time series' for each of the frequency sub bands are shown. Both the variations in time and in frequency are unusual relative to typical manmade non-thermal sources. Radar signals tend to occur as sharp, isolated pulses in time [*Ruf et al, 2006*]. Communication signals tend to maintain a steady level while present (Fig. S2). Both of these signal types tend to be very localized in frequency. The kurtosis observed on 8 June, on the other hand, is "bursty" and erratic over time in all eight sub bands to varying degrees. Typical non-thermal values for the kurtosis during this period range between 3.5 and 4.5. This represents 15- to 50- σ deviations from their nominal thermal value and can only be explained by non-thermal sources.

For comparison, the power of the signal (its second moment) is also shown in Fig. 2. There is evidence of only an extremely weak correlation between the variations in power and kurtosis. The correlation is weak because the power varies with the alignment between the Mars disk and the antenna beam, and with instrument gain. Fluctuations in the kurtosis, on the other hand, are immune to these effects, enabling extremely low-level non-thermal radiation to be detectable.

The first time that non-thermal radiation was detected, on 8 June 2006 at 19:14 UTC, the coordinates of the sub-Earth point on Mars were (15.71N, 216.29W). When the observations of non-thermal radiation ended at 22:40 UTC, the coordinates were

(15.74N, 267.38W). Non-thermal radiation was most intense at 19:14–19:21 and 21:50–22:09 UTC. MOC imaged a deep dust storm in this region during an overpass at 23:08 UTC. The storm centered on coordinates (31.17N, 226.08W) as shown in Fig. 2. The storm covers an area of $\sim 150,000 \text{ km}^2$ and is $\sim 35 \text{ km}$ deep based on the analysis of its image and the length of its shadow on the surface. It was located on the Earth facing side of Mars during our observations, within about 30° from the center of the disk. Thus, this dust storm is probably the source of the non-thermal radiation.

3. Spectral Analysis of Observations

Samples of the kurtosis were taken every 4.2 ms throughout the experiment. Its alias-free spectrum can be computed up to a maximum frequency of 110 Hz. A sample of the spectra of the kurtosis and the power of the microwave radiation is shown in Fig. S3. The spectrum of the kurtosis of the radiation contains a number of prominent peaks that are analyzed in more detail below. These features are present in the kurtosis over the entire period in which non-thermal radiation was detected. The spectrum of the power of the radiation contains one spectral feature at 27.8 Hz, also present in the kurtosis spectrum, and a strong peak at 60.0 Hz (ubiquitous with power measurements but absent from the kurtosis) that is likely caused by variations in the instrument gain.

An example of the time varying spectrum of the kurtosis is shown in Fig. 3. It contains prominent peaks at frequencies that are integer multiples of three fundamental frequencies. Table 1 summarizes these frequencies, with the harmonic amplitudes normalized by that of the fundamental frequency. The 2nd, 4th and 7th harmonics of the fundamental frequency $f_1 = 9.6 \text{ Hz}$ are present, along with the 2nd and 3rd harmonics of

both $f_2 = 27.8$ Hz and $f_3 = 31.7$ Hz. The 3rd, 5th and 6th harmonics of f_1 are not unambiguously seen in the spectrum. Higher harmonics of f_2 and f_3 may be present but are above the aliasing threshold and cannot be resolved. Fig. 3 demonstrates that the relative magnitudes of the different harmonics vary over time. It also reveals that the non-thermal activity tends to occur in alternating bursts and lulls.

4. The source of the microwave emissions

It is likely that electrical activity in the dust storm shown Fig. 1 is the source of the observed non-thermal radiation because collisions of sand and dust particles with each other and the surface are known to produce charge transfer [Stow, 1969; Schmidt *et al.*, 1998; Renno and Kok, 2008; Kok and Renno, 2009]. Electric discharges resulting from charge separation in the dust storm would produce non-thermal radiation [Melnik and Parrot, 1998; Farrell *et al.*, 1999; Renno *et al.*, 2003]. These electric discharges could occur on microscopic scales between colliding dust/sand particles [Renno *et al.*, 2003], on the scale of the saltation layer (~ 1 m) [Kok and Renno, 2009], or on the scale of the dust storm (~ 1 -35 km) [Stow, 1969; Melnik and Parrot, 1998; Farrell *et al.*, 1999; Renno *et al.*, 2004].

While electric discharges of various scales could contribute to the observed non-thermal radiation, the fact that the radiation is only observed for a few minutes, disappears, and then reappear at intervals ranging from minutes to hours (Fig. 3 and S4) suggests that micro-discharges are not the source of the emission, because they would occur continuously. Moreover, electric discharges are unlikely to occur in the saltation layer because discharge on its scale (~ 1 m) requires electric fields at least a few times

larger than predicted in saltation [Kok and Renno, 2009]. However, large-scale discharges in the dust storm could occur because conventional electric breakdown [Raizer, 1997] of the martian air at length scales of $\sim 1\text{-}35$ km requires electric fields of $\sim 15\text{-}25$ kV/m, which is smaller than what is predicted in dust storms [Melnik and Parrot, 1998; Kok and Renno, 2009]. Moreover, even smaller electric fields could produce runaway breakdown [Gurevich et al., 1992].

It follows from the above discussion that the non-thermal microwave radiation we observed was likely produced by large-scale (i.e., storm-scale or ~ 35 km) electric discharges in the dust storm shown in Fig. 1. Figure 3 shows that the emission of non-thermal radiation occurs in bursts lasting a few minutes. This suggests that, once large-scale discharges are initiated, they trigger new discharges. This behavior of networks of weakly coupled limit-cycle oscillators [Strogatz, 2000] has been observed in terrestrial lightning [Yair et al., 2006]. Once initiated, this process would stop only after the dust storm was substantially discharged. Moreover, it would not occur again until the storm was recharged. Thus, the interval between non-thermal emission events is indicative of the recharging time scale of the dust storm. This hypothesis also provides a plausible explanation for the spectral peaks observed in the kurtosis spectrum, as discussed below.

5. Modulation of the non-thermal radiation

Table 1 and Fig. 3 show that the observed non-thermal radiation is modulated by processes with frequencies $f_1 = 9.6$ Hz, $f_2 = 27.8$ Hz and $f_3 = 31.7$ Hz. These frequencies are within the range predicted for the three lowest resonant modes of the spherical cavity formed by the martian surface and its ionosphere [Schumann, 1952]. The frequency of

these fundamental modes of the Mars Schumann Resonance (SR) depends on a number of physical parameters, such as the height and conductivity profile of the martian atmosphere, ionosphere and surface. Their frequencies are predicted to be $f_1 = 7-14$ Hz, $f_2 = 13-26$ Hz and $f_3 = 19-38$ Hz [Yang *et al.*, 2006]. Two of the three fundamental frequencies of the spectrum of the kurtosis that we measured are within this range of values, with f_2 being slightly outside the predicted range. What is puzzling is that the martian SR appears to modulate the non-thermal radiation emitted by large-scale electric discharges. This is an unexpected result not observed before. We speculate on the reasons for this modulation next.

We hypothesize that perturbations of electric fields by the first three fundamental modes of the SR trigger the large-scale electric discharge that produces the non-thermal microwave radiation. These electric discharges in turn excite SR that triggers new electric discharges as suggested by Ondrášková *et al.* [2008]. This is analogous to the triggering of terrestrial lightning by perturbations from nearby discharges [Yair *et al.*, 2006; Strogatz, 2000] and the coherent excitation of SR by separate lightning discharges in a single thunderstorm [Ondrášková *et al.*, 2008]. In order to quantify this hypothesis, we estimate the amplitude of the electric field of SR excited by electric discharges in the dust storm shown in Fig. 1. Wait [1996] shows that the amplitude of the vertical component of the electric field produced by SR forced by incoherent discharges in an idealized spherical cavity is

$$E_z^{SR} \propto \frac{\overline{M}}{4a^2 \varepsilon \omega h \Delta t}, \quad (1)$$

where \overline{M} is the root mean square of the change in the vertical charge dipole moment in the time interval Δt , a is the planet radius, ε is the electric permittivity of air, ω is the SR

oscillation frequency, and h is the height of the ionosphere. Taking $E_{\max} \sim 20$ kV/m as the upper limit to the nearly critical (close to the breakdown value) electric field amplitude, between the surface and the top of the dust storm, an upper limit to the total charge in the storm is given by

$$Q_{Max} \approx A \varepsilon E_{Max}, \quad (2)$$

where $A \sim 150,000$ km² is the area covered by the dust storm and $\varepsilon \approx 8.85 \times 10^{-12}$ F/m is the electric permittivity of the martian air (\sim free space). Since the height of the dust storm is $z_{st} \approx 35$ km, the maximum charge moment of the storm is then $M_{Max} = z_{st} Q_{Max} \approx 10^9$ C m. If the dust storm were completely discharged in the minute long bursts seen in the kurtosis, the averaged rate of charge transfer squared would be 10^{16} (C m)²/s. For comparison, the typical root mean squared moment change of each lightning flash in terrestrial thunderstorms is about 1.6×10^5 C m and the average rate of vertical charge transfer squared is 1.7×10^{11} (C m)²/s [Heckman *et al.*, 1998]. Taking the upper limit in which the charge of the storm is transferred to the ground by incoherent lightning discharges in minute-long bursts suggested by the kurtosis (see Figure 3), we find that

$$\frac{E_{Mars}^{SR}}{E_{Earth}^{SR}} : \left[\frac{\left(\frac{\overline{M}}{\Delta t} \right)_{Mars}}{\left(\frac{\overline{M}}{\Delta t} \right)_{Earth}} \right] \left[\frac{a_{Earth}^2}{a_{Mars}^2} \right] \left[\frac{\varepsilon_{Earth}}{\varepsilon_{Mars}} \right] \sim 10^3 \left[\frac{\varepsilon_{Earth}}{\varepsilon_{Mars}} \right]. \quad (3)$$

This suggests that the amplitude of the electric field of martian SR could be orders of magnitude larger than that of terrestrial SR. Coherent discharges on Mars could produce even larger electric fields. Therefore, it is possible that SR works as a switch that triggers electric discharges in martian dust storms and therefore modulates the non-thermal microwave radiation produced by them. We show below that the fact that the spectrum of

the kurtosis contains some harmonics of the SR frequencies, but not others, supports this idea.

Suppose there exists a threshold value of the large-scale electric field above which non-thermal radiation is emitted. Variations of the total electric field above and below that threshold, caused by its time varying component from the modes of the SR, would act as an on/off switch for the non-thermal radiation. The following simple model describes the observed modulation. Let $x(t)$ be the state of the on/off switch that enables non-thermal radiation. Then

$$x(t) = \begin{cases} 1 & \text{if } 1 + \cos(2\pi f_o t) > x_{thresh} \\ 0 & \text{if } 1 + \cos(2\pi f_o t) < x_{thresh} \end{cases} \quad (4)$$

where f_o is the SR fundamental frequency and x_{thresh} is a number between 0 and 2 that represents the critical threshold value of the electric field. The Fourier series spectrum of $x(t)$ is given by

$$X(f) = \sum_{n=-\infty}^{\infty} c_n \delta(f - n f_o), \quad (5)$$

where $\delta(f)$ is the Dirac delta function, f is the frequency, and c_n are the Fourier series coefficients of $x(t)$

$$c_n = \frac{1}{\pi n} \sin(\pi n d), \quad (6)$$

and d , the duty cycle; is the fraction of time during which $x(t) > x_{thresh}$.

This model produces harmonics of the fundamental frequencies (f_o) in which the relative magnitudes of their Fourier coefficients are very sensitive to the duty cycle. The relative magnitudes of the observed harmonics of $f_l = 9.6$ Hz (listed in Table 1) are, for example, consistent with a duty cycle of $d = 0.37$. In this case, the four largest harmonic

coefficients are c_1 , c_2 , c_4 and c_7 . If, however, the duty cycle is changed slightly to $d = 0.40$, then the largest coefficients become c_1 , c_2 , and c_3 . This reproduces the observed harmonics of $f_2 = 27.8$ Hz. However, no duty cycle can produce a 3rd harmonic magnitude that is significantly larger than that of the fundamental, which is what is observed for the $f_3 = 31.7$ Hz SR mode. Thus, the model of a simple on/off threshold is incomplete because it can predict most, but not the entire observed spectrum.

6. Conclusions

An innovative microwave radiometer detected the emission of non-thermal radiation by a martian dust storm. Non-thermal radiation was detected only when a 35 km deep martian dust storm was in the field of view of the radio telescope. The non-thermal radiation was emitted in minutes-long bursts during a period of about 3 hours. The kurtosis of the radiation contains significant spectral peaks at the fundamental frequency of the lowest three modes of the martian Schumann Resonance and some of their harmonics. Our calculations suggests that changes in the charge moment of the order of that expected in a deep martian dust storm can force Schumann Resonance with amplitudes that are orders of magnitude larger on Mars than on Earth. We show that if the amplitude of the Schumann Resonance is large enough to trigger new electric discharges, it can reproduce the observed kurtosis spectrum. The discovery of evidence of electric activity in martian dust storms has important implications for atmospheric chemistry, habitability, and preparations for human exploration [Atreya *et al.*, 2006; Kok and Renno, 2009].

Acknowledgements

The authors gratefully acknowledge the cooperation of the Jet Propulsion Laboratory and the use of their Deep Space Network (DSN) facility. The engineering portion of this project was partially funded by NASA grant NNG05GL97G and the science by NSF award ATM 0622539.

References

- Delory, G., et al. (2006), Oxidant enhancement in martian dust devils and storms: Storm electric fields and electron dissociative attachment, *Astrobiology*, 6(3), 451-462.
- De Roo, R., S. Misra and C. Ruf (2007), Sensitivity of the Kurtosis Statistic as a Detector of Pulsed Sinusoidal RFI. *IEEE Trans. Geosci. Remote Sens.*, **45**(7), 1938-1946.
- Farrell, W.M., M.L. Kaiser, M.D. Desch, J.G. Houser, S.A. Cummer, D.M. Wilt and G.A. Landis (1999), Detecting electrical activity from Martian dust storms. *J. Geophys. Res.*, **104**(D2), 3795-3801.
- Gurevich A. V., G. M. Milikh, and R. Rousseldupre (1992), Runaway electron mechanism of air breakdown and preconditioning during a thunderstorm, *Phys. Lett. A*, 165 (5-6), 463-468.
- Huang, E., E. Williams, R. Boldi, S. Heckman, W. Lyons, M. Taylor, T. Nelson, C. Wong (1999), Criteria for sprites and elves based on Schumann Resonance observations. *J. Geophys. Res.*, **104** (D), 16,943-16,964
- Kok, J. F., and N. O. Renno (2008), Electrostatics in wind-blown sand, *Phys. Rev. Lett.*, **100** (1), 014501, doi:10.1103/PhysRevLett.100.014501.
- Kok, J.F., and N.O. Renno (2009), Electrification of wind-blown sand on Mars and its implications for atmospheric chemistry, *Geophys. Res. Lett.*, **36**, L05202, doi:10.1029/2008GL036691.
- Melnik, O., and M. Parrot, 1998. Electrostatic discharge in Martian dust storms. *J. Geophys. Res.*, **103**, 29,107.

- Ondrášková, A., J. Bór, S. Ševčík, P. Kostecký and L. Rosenberg (2008), Peculiar transient events in the Schumann resonance band and their possible explanation. *J. Atmos. Sol. Terr. Phys.*, 70, 937-946, doi:10.1016/j.jastp.2007.04.013.
- Raizer, Y. P. (1997), *Gas Discharge Physics*, Springer, Berlin.
- Renno, N.O., V. Abreu, J. Koch, P.H. Smith, O. Hartogenesis, H.A.R. de Bruin, D. Burose, G.T. Delory, W.M. Farrell, M. Parker, C.J. Watts, A. Carswell (2004), MATADOR 2002: A field experiment on convective plumes and dust devils. *J. Geophys. Res.*, **109**, E07001, doi:10.1029/2003JE002219.
- Renno, N.O., A.S. Wong, S.K. Atreya, I. de Pater, M. Roos-Serote (2003), Electrical discharges and broadband radio emission by Martian dust devils and dust storms. *Geophys. Res. Lett.*, **30**, doi:10.1029/2003GL017879.
- Renno, N. O., and J. F. Kok (2008), Electrical activity and dust lifting on Earth, Mars, and beyond, *Space Sci. Rev.*, 137 (1-4), 419-434, doi:10.1007/s11214-008-9377-5.
- Ruf, C.S., S. M. Gross and S. Misra (2006), RFI Detection and Mitigation for Microwave Radiometry with an Agile Digital Detector. *IEEE Trans. Geosci. Remote Sens.* , **44**(3), 694-706.
- Schmidt, D.S., R. A. Schmidt, and J. D. Dent (1998), Electrostatic force on saltating sand. *J. Geophys. Res.*, **103**(D8), 8997-9001.
- Schumann, W.O. (1952), On the free oscillations of a conducting sphere which is surrounded by an air layer and the ionosphere shell. *Z. Naturforschung*, 72, 250-252.
- Stow, C.D. (1969), Dust and sand storm electrification, *Weather*, **24**,134-137.
- Strogatz, S.H. (2000), From Kuramoto to Crawford: exploring the onset of synchronization in populations of coupled oscillators. *Physica, D*, 1-20.

Wait, J. R. (1996), *Electromagnetic Waves in Stratified Media*, IEEE Press, Piscataway, N.J.

Yair, Y. et al., (2006), Evidence for synchronicity of lightning activity in networks of spatially remote thunderstorms, *J. Atmos. Sol.-Terr. Phys.*, 68(12), 1401-1415.

Yang, H., V. P. Pasko and Y. Yair (2006), Three-dimensional finite difference time domain modeling of the Schumann resonance parameters on Titan, Venus and Mars. *Radio Science*, **41**(RS2S03).

	frequency (Hz)	magnitude (normalized)	frequency (Hz)	magnitude (normalized)	frequency (Hz)	magnitude (normalized)
Fundamental	9.6	1.00	27.8	1.00	31.7	1.00
2 nd	19.2	0.91	55.7	0.33	63.4	note 1
3 rd	28.8	note 1	83.5	0.22	95.1	2.90
4 th	38.4	0.41	note 2		note 2	
5 th	48	note 1	note 2		note 2	
6 th	57.6	note 1	note 2		note 2	
7 th	67.2	0.83	note 2		note 2	

Note 1. These harmonics were not unambiguously present in the spectrum;

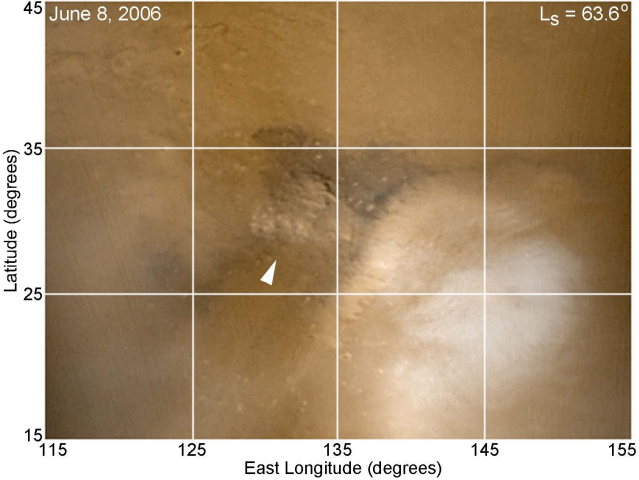
Note 2. These harmonics are above the range of observable frequencies.

Table 1. Harmonic components of kurtosis of the data collected during the 8 June 2006 dust storm in sub band #4 at 8480 MHz. Magnitudes are relative to the fundamental frequency for that particular harmonic.

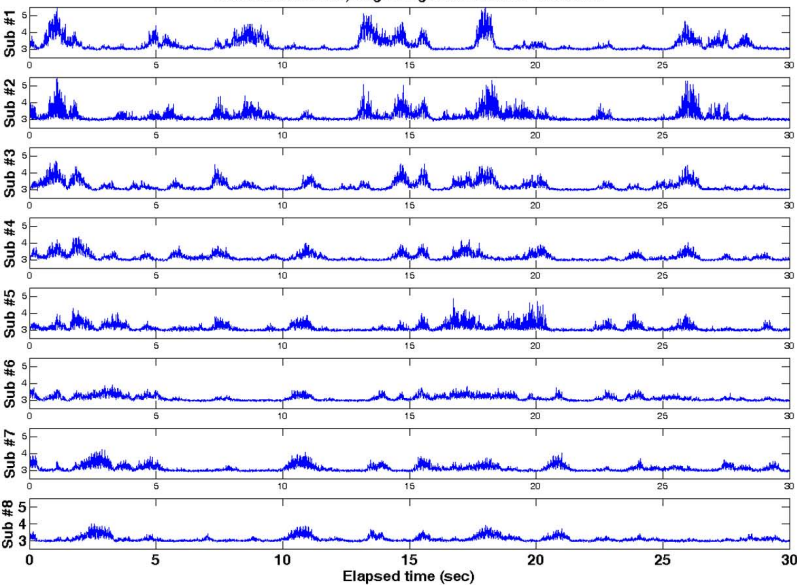
Figure 1. Dust storm imaged by the Mars Orbiter Camera in a region just NW of Elysium Mon (31.2N, 133.9E) on 8 June 2006. The false-color composite was generated from red and blue filter wide-angle images (S19-00652 and S19-00653). The storm covers about 150,000 km². Shadows on NE side of storm indicate that the dust cloud reaches at least 35 km above the surface. The white arrow indicates the location of the storm. The white area in the lower right is an orographic water-ice cloud over Elysium Mons. This storm only persisted for a Sol only.

Figure 2. Kurtosis (top) and power (bottom) time series of Mars microwave emission measured between 19:20:00 and 19:20:30 UTC on 8 June 2006 in eight spectral sub bands between 8470 and 8490 MHz. Non-thermal emission is indicated by the departure of the kurtosis from a value of 3.

Figure 3. Time series of power spectrum of kurtosis for data collected over 10 minutes on 8 June 2006 beginning at 21:58 UTC while dust storm was visible from the DSS-13 site. Spectrum is computed every 1 s from ± 5 s of data from sub band #4 at 8480 MHz, resulting in 0.1 Hz spectral resolution. Color bar is linearly proportional to power spectral density.



Mars Kurtosis Obs, Beginning 8 Jun 2006 at 19:20 UTC



Mars Power Obs, Beginning 8 Jun 2006 at 19:20 UTC

